

Phagocytosis and Phagosomal Fate of Surface-Modified Microparticles in Dendritic Cells and Macrophages

Lars Thiele,¹ Hans P. Merkle,¹ and Elke Walter^{1,2}

Received October 7, 2002; accepted November 1, 2002

Purpose. We compared cationic, polyamine-coated microparticles (MPs) and anionic, protein-coated MPs with respect to their phagocytosis and phagosomal fate in dendritic cells (DCs) and macrophages (MΦ).

Methods. Polystyrene MPs were surface modified by covalent coupling with fluorescein isothiocyanate-labeled polyamines or proteins. Phagocytosis of MP and the pH of their intracellular microenvironment was assessed in human-derived DCs and MΦ in a fluorescence plate reader. Visualization of MP phagocytosis in DCs was performed by transmission electron microscopy.

Results. Phagocytosis of bovine serum albumin-coated MPs was low with significant differences between DC and MΦ, whereas phagocytosis of IgG-coated MPs was significantly enhanced in both cell types. Phagocytosis of both particle types resulted in an acidified phagosomal microenvironment (pH 4.6–5.1). In contrast, cationic, polyamine-coated MPs were equally phagocytosed by DCs and MΦ to a high extent and showed lower degrees of acidification (pH 6.0–6.8) in the phagosomal microenvironment. Transmission electron microscopy examination demonstrated all phagocytosed particles to be surrounded by a phagosomal membrane, which was more tightly apposed to the surface of cationic MPs and more loosely to bovine serum albumin-coated MPs.

Conclusion. Phagocytosis of cationic, polyamine-coated MPs is suggested to lead to diminished phagosomal acidification. Thus, cationic MP are potential carriers that may display beneficial features for the intracellular delivery of immunomodulating therapeutics and their protection against lysosomal degradation.

KEY WORDS: dendritic cells; macrophages; surface-modified microparticles; phagocytosis, intracellular fate.

INTRODUCTION

The internalization of particles in the micrometer range, i.e., microparticles (MP), is a special feature of phagocytic cells and has recently received high interest to enable targeted delivery of therapeutics into dendritic cells (DCs) and macrophages (MΦ; 1–3). DCs and MΦ are professional antigen-presenting cells and, thus, represent targets for the delivery of vaccines (4,5). Particularly, DC were found to elicit T-cell responses that were up to 3000 times stronger than those observed with MΦ. In addition, DCs feature unique capabilities to modulate the immune system toward immunity or tolerance (6,7). Upon phagocytosis, antigens associated to MPs have been shown to elicit strong cytotoxic T-cell responses (8,9), being a consequence of their access to the MHC class I pathway of presentation (10–13). In this context, the advan-

tage of MP-associated antigens over soluble antigens appears to result from at least the following two factors: 1) the opportunity to internalize large quantities of antigen when embodied in MP, and 2) their prolonged release and thus more efficient presentation as compared with a short-lived bolus of antigen delivered in soluble form.

Phagocytosis of MPs as well as the presentation of MP-associated antigens have been demonstrated to be strongly influenced by the chemical and physical nature of the MPs (3,14–16). To initiate phagocytosis, the MP surface needs to stimulate binding to the cellular membrane, which subsequently sets off internalization into the cell. Recent studies revealed that particularly MPs displaying a positive surface charge were subject to efficient phagocytosis by both MΦ and DCs (14,17). Interestingly, although the phagocytosis activity of DCs is generally considered to be lower than that of more efficient phagocytes, such as MΦ, the phagocytosis of cationic MPs by DCs has been demonstrated to measure up with MΦ (4,5,14,18,19).

Phagocytosis leads to the intracellular entrapment of MPs in phagosomes, which mature under the influence of acidification, resulting from their fusion with lysosomes by forming so-called phagolysosomes (20). The process of phagosome maturation has been shown to relate to the degree of apposition of the phagosomal membrane to the entrapped MPs (20–22). There are two alternatives. The first is hydrophilic MPs, entrapped in spacious phagosomes with the phagosomal membrane and in loose contact to the MP surface, are subjected to rapid fusion with lysosomes. The second is mycobacteria or hydrophobic latex particles were observed to resist rapid fusion with lysosomes, which was suggested to be caused by their tight apposition to the phagosomal membrane (21).

MPs carrying positively charged surfaces may be obtained by coating them with cationic excipients owing to the protonation of their amino groups (23–25). Because of their buffer capacity, these compounds have been suggested to delay phagosomal acidification (26) and subsequently cause impaired fusion with lysosomes or even deliver particle-associated antigens to the cytosol. Cytosolic delivery of antigens or DNA vaccines represents an important prerequisite for antigen presentation via the major histocompatibility complex class I to specifically stimulate cytotoxic T lymphocyte response.

For the first time, this study aims to investigate the influence of positively charged MPs on their phagocytosis and subsequent intracellular fate in DCs and MΦ. Moreover, for comparison with positively charged MPs, we also studied MPs with various other surface modifications that were expected to cause either unspecific or receptor-mediated phagocytosis. The various MP surfaces were characterized for charge and hydrophobicity, and the phagocytosis of the respective MPs was assessed with human blood-derived DCs and MΦ by using an automated fluorescence plate reader. By the same methodology, we determined the intracellular pH in the microenvironment of phagocytosed MP using the pH-dependent intensity of a fluorescence signal to probe the phagosomal pH. Additionally, we used transmission electron microscopy (TEM) to study the mechanisms of phagocytosis and assess the residence of phagocytosed MP.

¹ Department of Applied BioSciences, Swiss Federal Institute of Technology Zurich (ETH), Winterthurerstrasse 190, CH-8057 Zurich, Switzerland.

² To whom correspondence should be addressed. (e-mail: elke_walter@gmx.net)

MATERIALS AND METHODS

Materials

Poly-L-lysine hydrobromide (PLL 29, mean molecular weight [MW] 29 kDa and PLL 99, mean MW 99 kDa), fluorescein isothiocyanate (FITC), bovine serum albumin (BSA), human IgG, and phosphate-buffered saline (PBS, pH 7.4) were purchased from Sigma, Buchs, Switzerland. Polyethylenimine (PEI, MW 600,000–1,000,000) was obtained from Fluka, Buchs, Switzerland. Trypan blue was obtained from Merck AG, Darmstadt, Germany. Materials for cell culture experiments were obtained from Life Technologies, Basel, Switzerland. All other chemicals used were of analytical grade unless otherwise specified and obtained from Fluka, Buchs, Switzerland.

Surface Modification of MPs

Surface modified MPs were obtained by covalent conjugation of carboxylated polystyrene MPs (1.0 μm in diameter, Polybead™, Polysciences, Eppelheim, Germany) with IgG, BSA, PLL, or PEI (50 $\mu\text{g}/\text{mg}$ MP) using the carbodiimide method (data sheet #238 C, Polysciences, Eppelheim, Germany). To separate coated MPs from unbound coating material, the MPs were centrifuged (6 min, 21,000 \times g, 20°C) and subsequently washed three times in PBS, pH 7.4, to remove unbound material. The amount of unbound coating material was determined in the supernatant upon conjugation with fluorescamine (0.3 mg/mL in acetone) according as described previously (27). Quantitative analysis was performed by using an automated plate reader (Fluoro Count, Canberra Packard, Frankfurt, Germany; filters: 360/460 nm).

FITC Labeling of Coating Material and MPs

Soluble IgG, BSA, PLL, and PEI or surface-modified MPs, respectively, were fluorescence-labeled with FITC in carbonate buffer (0.5 M, pH 9.5) according to Arvinte *et al.* (28). FITC-labeled soluble IgG, BSA, PLL, and PEI were purified by dialysis in PBS using a Spectra/Por® Membrane (MWCO 3500, Spectrum Medical Industries, Inc., Hollister, CA, USA). FITC-labeled surface-modified MP were separated from excess FITC by repeated washings and subsequent centrifugation.

Determining the Surface Charge of MPs by ζ -Potential Measurement

The ζ -potentials of various MPs were determined using a Zeta-Meter System 3+ (ZM3+ 331, Zeta-Meter, Inc., Staunton, VA, USA). Three samples of each MP type were measured at 25°C in double distilled water containing 0.01 M NaCl.

Determining the Hydrophobicity of MP by the Rose Bengal Assay

Different amounts of MP (0.3–1.8 mg/mL, corresponding to 5.5×10^8 – 3.3×10^9 particles per mL) were suspended in a solution of 20 $\mu\text{g}/\text{mL}$ Rose Bengal in 0.1 M phosphate buffer of pH 7.4. Samples were incubated at room temperature for 3 h in the dark, centrifuged at 21,000 \times g, and the amount of non-adsorbed Rose Bengal in the supernatant was determined by

using an automated fluorescence plate reader (filters: 530/590 nm). The partition quotient was calculated by dividing the amount of Rose Bengal bound on the MP surface by the amount of Rose Bengal remaining in the dispersion medium. Plotting of partition quotient against the total surface area of the MP resulted in straight lines. The slope of such lines was taken as parameter for the hydrophobicity of the MP surface (29). Slopes were calculated by linear regression analysis.

Fluorescence Intensity of FITC-Labeled Coat Materials as a Function of pH

Purified FITC-labeled coating materials were dissolved at various pH (pH 2–5.5 in 0.5 M citrate buffer, pH 5.5–10 in PBS). The fluorescence intensity was measured using an automated fluorescence plate reader (filters: 485/530) and expressed as relative fluorescence intensity with 100% fluorescence at pH 7.4.

M Φ and DC Cell Cultures

DCs and M Φ were obtained from human peripheral blood monocytes according to Sallusto *et al.* (30). Briefly, peripheral blood monocytes were isolated from buffy coats (Bloodbank Zurich, Switzerland) by density gradient centrifugation on Ficoll-Paque (Pharmacia Biotech). Peripheral blood monocytes were resuspended in RPMI 1640 supplemented with 10% heat inactivated (pooled) human serum (Bloodbank Zurich, Switzerland) and then allowed to adhere for 2 h in culture flasks (25 cm^2). Nonadherent cells were removed and adherent cells were cultured in RPMI 1640 medium supplemented with 5% heat inactivated (pooled) human serum in the presence of 1000 IU/mL interleukin-4 (Sigma) and 50 ng/mL GM-CSF (R+D Systems) for the generation of DCs, whereas M Φ were obtained without any additional supplements (31). For phagocytosis studies, cells were mechanically removed from the flasks during the first day of culture and reseeded in 96-well plates. Cultures were kept at 37°C in 5% CO₂ humidified atmosphere for 7–10 days before used for further experiments.

Characterization of DCs and M Φ

Surface antigen expression of DCs and M Φ was analyzed by flow cytometry (32). For further identification of DCs, the cells were also challenged with lipopolysaccharide (LPS; 1 $\mu\text{g}/\text{mL}$) for 48 h to induce DC maturation. The cells were incubated (45 min, 4°C) with each of the following primary anti-human antibodies: CD11b (Mac-1, ICRF44, Pharmingen; 44), CD14 (Clone UCHM-1, Sigma), CD83 (Clone HB15e, Pharmingen), CD86 (B70/B7-2, Clone IT2.2, Pharmingen), MHC I (HLA-ABC, Clone W6/32, Dako), and MHC II (HLA-DP, DQ, DR, Clone CR3/43, Dako). In a similar way controls were performed by using mouse isotype control IgG2a (UPC-10, Sigma). The cells were washed three times and subsequently incubated with the secondary antibody (anti-mouse IgG R-Phycoerythrin conjugate, Sigma) for 45 min at 4°C. Afterwards, the cells were washed again three times and then transferred to FACS tubes and analyzed on a FACScan type Becton Dickinson. The presence of CD14 and the absence of CD83 after LPS stimulation is regarded to be characteristic for M Φ , whereas the presence of CD11b, the absence of CD14 and the upregulation of CD83 and CD86

after LPS stimulation is characteristic for DC (6,32). According to these criteria, more than 90% of the cells were identified as DC or MΦ, respectively.

Cell Viability and Trypan Blue Quenching

Trypan blue quenching simultaneously allows the determination of cell viability and phagocytosis activity (14). Cell viability was checked by trypan blue exclusion (1% in PBS pH 7.4) as described elsewhere (14,33). When used as a solution of 250 μg/mL in citrate buffer (pH 4.4), trypan blue has been demonstrated to completely quench extracellular fluorescence of FITC as described in a previous study in detail (14). In addition, penetration of trypan blue into necrotic cells typically leads to quenching of intracellular fluorescence. Thus, the recorded fluorescence strictly originates from phagocytosed MP in viable cells only.

Determination of MP Phagocytosis and Intracellular pH

DCs and MΦ were cultured in 96-well plates at 10^4 cells per well for 10 days. For phagocytosis studies, the medium was replaced by 50 μL of MP dispersed in HEPES buffer (0.2 M, pH 7.4) containing 1 mM Ca^{2+} ($3.3 \cdot 10^8$ MP/mL). Cells were incubated at pH 7.4, either 4 or 37°C, for 4 h. The subsequent measurement of fluorescence intensity was performed at room temperature by using an automated plate reader (filters: 485/530). The following parameters were used:

- F_{all} : Fluorescence intensity of all MP incubated in the presence of cells at 4°C. At this temperature phagocytosis was blocked to allow determination of F for all MP in the extracellular milieu (pH 7.4).
 F_{37} : Fluorescence intensity of all MP incubated in the presence of cells at 37°C.
 F_{intra} : Measured after quenching with trypan blue, representing the fluorescence intensity of all phagocytosed, intracellular MP.
 P_a : Number of MP per well.
 C : Number of cells per well.

Calculation of MP Uptake

Because of the pH sensitivity of the fluorescence label, its reduced intracellular fluorescence in a low pH environment can be compensated as follows:

$$\begin{aligned} \text{Fluorescence intensity of a single} \\ \text{particle:} & F_{\text{MP}} = F_{\text{all}}/P_a \\ \text{Amount of nonphagocytosed} \\ \text{extracellular MP at 37°C:} & F_{\text{extra}} = F_{37} - F_{\text{intra}} \\ \text{Number of extracellular MP:} & P_e = F_{\text{extra}}/F_{\text{MP}} \\ \text{Number of intracellular MP:} & P_i = P_a - P_e \end{aligned}$$

Average number of MP phagocytosed per cell: P_i/C

Calculation of Intracellular pH in the Microenvironment of Phagocytosed MPs

The pH-dependent fluorescence intensity of phagocytosed MPs relates to P_i and the difference between extracellular and intracellular pH as previously used by (34,36–38):

$$\begin{aligned} \text{Change in fluorescence intensity} \\ \text{of } P_a \text{ after phagocytosis:} & F_{\text{phago}} = F_{\text{all}} - F_{37} \\ \text{Fluorescence intensity of } P_i \text{ at} \\ \text{pH 7.4:} & F_{7.4} = F_{\text{intra}} + F_{\text{phago}} \\ \text{Remaining relative fluorescence} \\ \text{intensity of } P_i: & F_{\text{remain}\%} = F_{\text{intra}}/F_{7.4} \cdot 100 \end{aligned}$$

By means of the fluorescence intensity of various FITC-labeled polymers (PLL, PEI, IgG, and BSA) as a function of pH, microenvironmental pH values can be derived from the experimentally obtained fluorescence intensities, i.e., $F_{\text{remain}\%}$. The respective profiles are depicted in Fig. 1 and are further described in the results section.

Microscopic Assessment of Phagocytosis

The intracellular fluorescence of very small numbers of MPs was below the detection limit of the fluorescence plate reader. Thus, phagocytosis of BSA-coated MPs by DCs was assessed by fluorescence microscopy (Axiovert 35, Zeiss, Oberkochen, Germany). Phagocytosis studies and subsequent quenching of extracellular MPs with trypan blue were performed as described above. The extent of phagocytosis was then monitored by using an inverted microscope (Axiovert 35, Zeiss, Oberkochen, Germany) equipped for fluorescence microscopy (excitation 450–490 nm, emission 520 nm). Data indicate the mean number of MPs counted in 150 representative cells per sample.

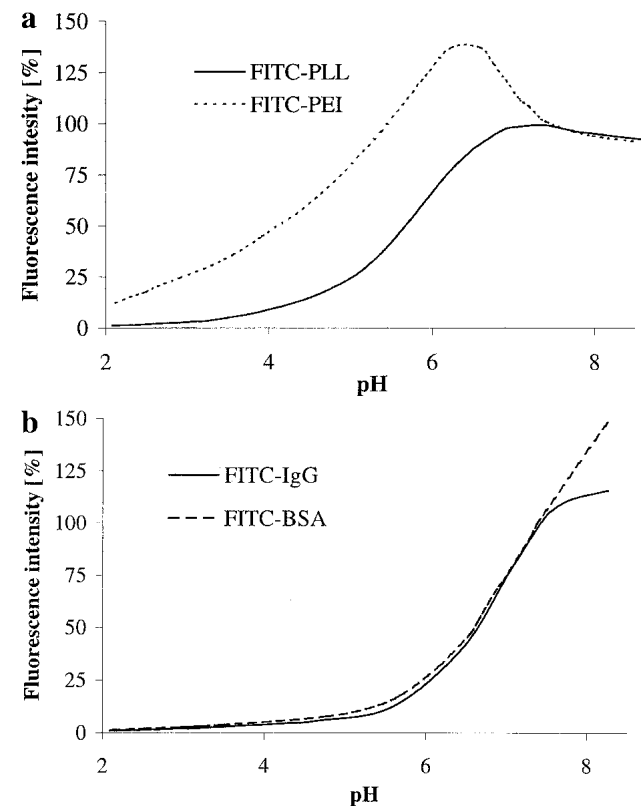


Fig. 1. Fluorescence intensity of FITC-labeled coating materials, (a) FITC-PLL and FITC-PEI, (b) FITC-BSA and FITC-IgG, as a function of pH. The fluorescence intensity is expressed in % was set to 100% at pH 7.4.

Processing of Cells for TEM

Cells were washed three times in Hank's balanced salt solution and resuspended in phosphate buffered 2.2% glutaraldehyde solution at pH 6.8. The cells were postfixed in 1% osmium tetroxide in 0.1 M sodium cacodylate buffer and contrasted in 0.5% uranyl acetate in 0.05 M maleate buffer. Dehydration was performed in a graded series of ethanol-water mixtures (v/v; 70, 80, 96, and 100%). Gradual replacement of ethanol was performed with propylene oxide before infiltration and embedding in epoxy resin. Ultrathin sections were cut using an ultramicrotome (Reichert, Vienna, Austria) and were collected on 200-mesh carbon-coated copper grids. After staining with uranyl acetate and counterstaining with lead citrate, samples were observed by TEM at 60 kV using a Phillips 300 (Phillips Electronic Instruments, Inc., New Hanover, NJ, USA).

RESULTS

Properties of Various Surface-Modified MPs

MPs displaying different surface properties were generated by covalent coating with either proteins (BSA or IgG) or polyamines (PEI or PLL; Table I). All surface modifications resulted in high coating efficiencies ranging from 15–30 $\mu\text{g}/\text{mg}$ MPs (equivalent to 2.6–5.2 ng/mm^2). Surface charges were determined by measuring the ζ -potentials. Polyamine-modified MPs displayed highly positively charged surfaces in the range of +45.7 to +38.2 mV, whereas protein-modified MP displayed negatively charged surfaces in the range of –16.9 to –21.1 mV (Table I). As a control, the surface charge of plain polystyrene MPs was practically neutral. Moreover, we determined the hydrophobicity of the various surface-modified MPs by the previously established Rose Bengal partitioning method (29,36). The method was modified and performed as a microassay. In principle, MPs dispersed in an aqueous medium were regarded as a two-phase system with the surface layer of the MPs as one phase and the dispersion medium as the second phase. Plotting of the partition coefficients of the dye against the total surface area of the microspheres yielded straight lines. The slopes represent arbitrary hydrophobicity values for the surface of the microspheres. As expected, plain polystyrene MPs displayed the highest hydrophobicity followed by BSA- and IgG-coated MPs (Fig. 2). The Rose Bengal partitioning method was not suitable for cationic surfaces because of ionic interactions with the negatively charged Rose Bengal. However, because of the high charge density of

Table I. Coating Efficiency and Surface Charge of Polyamine and Protein-Coated Microparticles

Type of coating	Coating efficiency ($\mu\text{g}/\text{mg}$)	ζ -potential (mV) ^a
PLL 29	29.8 \pm 1.2	+38.2 \pm 3.3
PLL 99	27.4 \pm 2.6	+42.0 \pm 3.5
Polyethylenimine	26.3 \pm 3.3	+45.7 \pm 4.1
IgG	14.5 \pm 1.9	–21.1 \pm 1.6
Bovine serum albumin	18.4 \pm 2.1	–16.9 \pm 1.2
Non-coated MPs	—	–0.8 \pm 1.5

^a Measured in 0.01 N NaCl; data are means of three samples \pm SD.

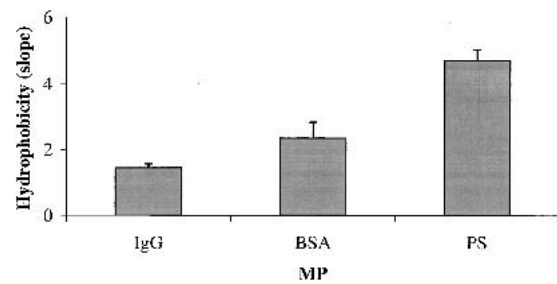


Fig. 2. Relative hydrophobicity of various surface-modified microparticles determined by the Rose Bengal adsorption assay. Data show the mean \pm SD ($n = 3$). Non-coated polystyrene microparticles (PS).

the polyamine coating, assumption of a rather hydrophilic surface is reasonable.

Assessment of Phagocytosis and Intracellular pH in the Microenvironment of Phagocytosed MP

We measured the phagocytosis of the various surface-modified MPs in human blood-derived M Φ and DCs by using an automated fluorescence plate reader. To not to change the surface properties of the MP as the result of serum protein adsorption, a serum-free incubation medium was used. Further studies are currently performed to assess the influence of serum protein adsorption on the phagocytosis of M Φ and DCs. The assessment of intracellularly located MPs requires surface- but not bulk-conjugated FITC to allow quenching of extracellular fluorescence by trypan blue (14). The pH-dependent fluorescence intensity of various FITC-derivatives is characterized as outlined in Fig. 1. Because the phagocytosed MPs may be exposed to an acidic intracellular environment as it occurs in phagosomes or phagolysosomes, the change in fluorescence intensity must be compensated to assess phagocytosis capacity. Furthermore, we used the pH-dependent fluorescence intensity to calculate the pH in the microenvironment of phagocytosed MPs. The change in pH was most pronounced between pH 4 and 7 (Fig. 1a and b) and, thus, the phagosomal pH can be determined depending on the state of phagosomal maturation (34,35,37,38).

Phagocytosis of the various surface-modified MPs was determined in DCs and M Φ (Fig. 3). BSA-coated MP with a negatively charged and comparatively hydrophilic surface were phagocytosed by DCs at a significantly lower degree than by M Φ . In contrast, phagocytosis of IgG-coated MP displaying analogous surface properties was much larger and at

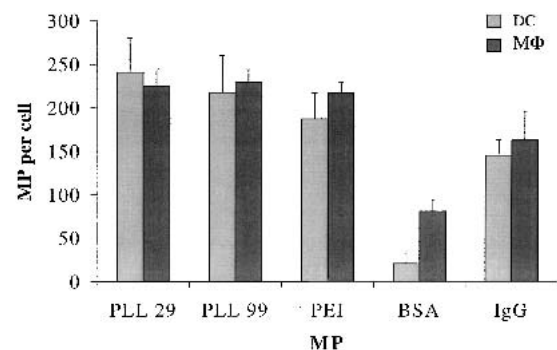


Fig. 3. Phagocytosis of various surface-modified microparticles by macrophages and dendritic cells. Data show the mean \pm SD ($n = 3$).

comparable efficiencies with both cell types. All cationic polyamine-modified MPs induced phagocytosis on the highest level in both DCs and MΦ (Fig. 3).

The pH in the microenvironment of phagocytosed MPs was probed using a pH-dependent fluorescent label conjugated to the various tested polyamine (PLL and PEI) or protein coatings (IgG and BSA). The relationships between the recorded fluorescence intensities and the pH of the tested polymers are depicted in Fig. 1, showing more or less sigmoidal relationships for PLL, IgG, and BSA.

An acidified microenvironment was found in the phagosomes of the IgG-coated MP in the range of pH 4.6 to 5.1, both in DC and MΦ (Table II). The low incidence of phagocytosis of BSA-coated MPs by DCs was below the detection limit of the fluorescence plate reader. Thus, information about the effect of BSA-coated MPs on the phagosomal pH in DCs is missing, but phagosomes of MΦ were shown to be similarly acidified as upon IgG-coated MPs. In contrast, the microenvironment of phagocytosed PLL-coated MPs was less acidic for both DCs and MΦ, i.e., pH 6.0–6.3 for both PLL coatings (Table II). The peak-shaped profile, which was found in the case of PEI led to two potential pH values of 6.0 and 6.8, both indicating a significantly increased microenvironmental pH compared with protein-coated MPs (Table II). In summary, our data may suggest diminished phagosomal acidification in the presence of polyamine-coated MPs vs. protein-coated MPs.

Mechanism of Phagocytosis and Intracellular Fate of the MP

We used TEM to compare the histology of the phagocytosis and the intracellular fate of cationic, polyamine-coated MPs with those of anionic, protein-coated MPs, both in DCs and MΦ. The objectives of these experiments were to distinguish between two hypotheses for the diminished acidification. Firstly, intraphagosomal buffering and or delay of phagosomal maturation may be continued. Secondly, polyamine-induced rupture of the endosomal membrane has been previously demonstrated to lead to the endosomal escape of PEI-associated material into the cytosol (26).

Previously, BSA-coated MPs have been demonstrated to be internalized into spacious phagosomes followed by a rapid fusion with lysosomes (21). In our study, PLL 99 and PEI-coated MPs were chosen as examples for cationic MP and compared with anionic, BSA-coated MP. As confirmed by TEM, the majority of the polyamine-coated MPs were inti-

mately engulfed by large pseudopods (Fig. 4a, arrows), resulting in a tightly apposed membrane covering the surface of the MPs (Fig. 4a, arrowheads). In some cases cationic MPs appeared to sink into the cells, especially for the sequential phagocytosis of several MPs in a row. Nonetheless, after phagocytosis cationic MPs were always enclosed by a tightly apposed membrane (Fig. 4b, arrowheads). In contrast, pseudopod formation was never observed upon phagocytosis of BSA-coated MPs, which appeared to sink into the cells as already observed in previous studies (21).

After 4 h, the vast majority of the polyamine and BSA-coated MPs were found to be enclosed by a phagosomal membrane (Fig. 5) with only a few exceptional polyamine-coated MPs, where such a membrane could not be clearly identified. BSA-coated MPs were mainly found in spacious phagosomes with large parts of the phagosomal membrane being distant from the surface of the MP (Fig. 5a). Only few MPs were found in phagosomes with a tightly apposed membrane (Fig. 5b). In contrast, the majority of PLL 99-coated MPs (Fig. 5c and d) and PEI-coated MPs (Fig. 5e and f) were engulfed in phagosomes with tightly apposed phagosomal membranes (Fig. 5c–f).

DISCUSSION

Cationic MPs have gained increasing interest as delivery systems to target phagocytic cells such as DC and MΦ (14,24,39–41). Their cationic surface charge has been demon-

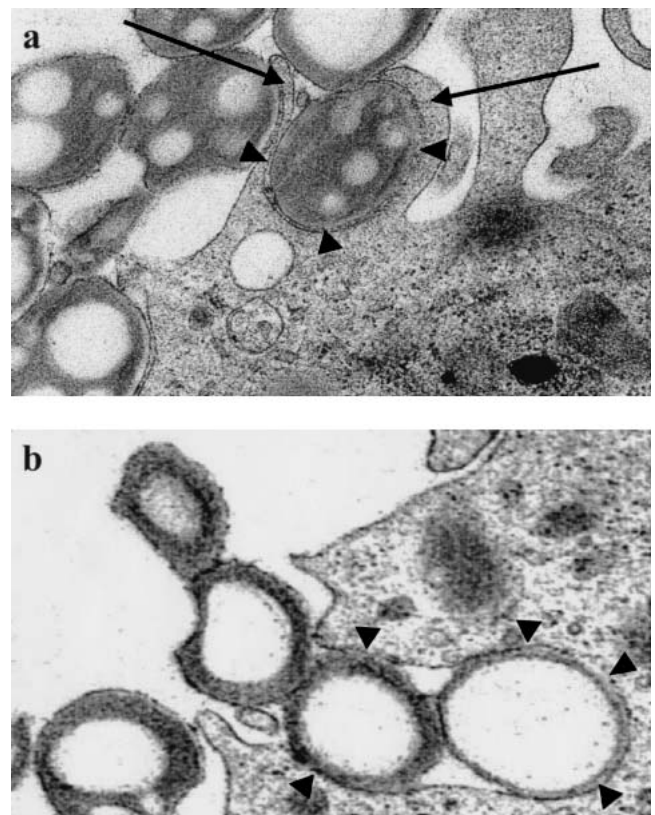


Fig. 4. Transmission electron microscopy of the phagocytosis of polyethyleneimine-coated microparticles (MPs) by dendritic cells. (a) The majority of MPs are internalized by the formation of pseudopods (arrows) or (b) in some cases by sinking into the cell. The cellular membrane is tightly adjoined to the MP surface (arrowheads).

Table II. Microenvironmental pH in the Phagosomes of Phagocytosed Microparticles Coated with Various Polyamines and Proteins

Type of coating	pH in DC ^a	pH in MΦ ^a
PLL 29	6.0 ± 0.1	6.1 ± 0.2
PLL 99	6.3 ± 0.2	6.1 ± 0.3
Polyethylenimine	6.0 ± 0.2 (6.8 ± 0.2) ^b	6.0 ± 0.2 (6.7 ± 0.2) ^b
IgG	5.1 ± 0.2	4.9 ± 0.1
Bovine serum albumin	n.d.	4.6 ± 0.4

^a Data represent means of three samples ± SD.

^b The peak-shaped profile of fluorescence intensity chart led to two potential pH values with the higher number given in parentheses (see Fig. 1).

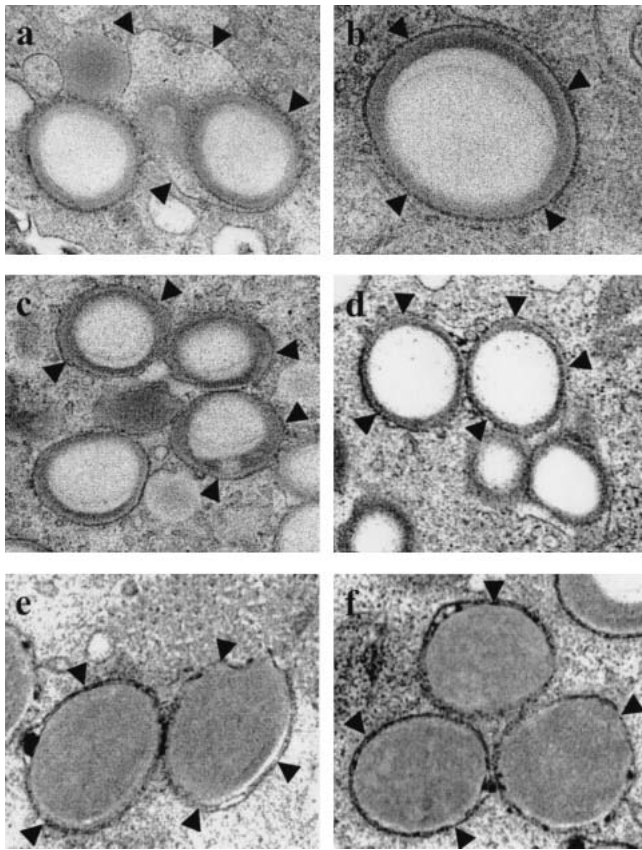


Fig. 5. Transmission electron microscopy of surface-modified MPs phagocytosed by dendritic cells after 4 h for (a, b) BSA-coated microparticles (MPs), (c, d) PLL 99-coated MPs, and (e, f) polyethyl-eneimine-coated MPs. MPs are located in phagosomes with the phagosomal membrane tightly adjoined to the MP surface (b-f) or in spacious phagosomes with large parts of the phagosomal membrane distant from the MP surface (a).

strated to strongly enhance phagocytosis by such cells (14). In this study, we investigated the degree of phagocytosis of various polyamine-coated MPs in comparison to protein-coated MPs, including an IgG-coating that was previously shown to elicit receptor-specific phagocytosis (42,43). In addition, we evaluated the mechanism of phagocytosis and the intracellular fate of internalized MPs by probing their microenvironmental pH in combination with electron microscopy. Cationic MPs were efficiently phagocytosed by DCs through extensive pseudopod formation and ended up in phagosomes displaying a tightly apposed membrane. The expected acidification of the phagosomal microenvironment was only found with protein-coated MPs, whereas the phagosomes containing polyamine-coated MPs turned out to be less acidic. Typically, low phagosomal acidification was always concomitant with tight engulfment by the phagosomal membrane.

Consistent with other studies, hydrophilic BSA-coated MPs were internalized at a comparatively low frequency by M Φ (41,44,45) and even more reduced by DC. The relatively low capacity of DC for nonspecific phagocytosis of foreign material has been demonstrated in previous studies (18,46,47). Whereas particle scavenging by M Φ was found to be highly efficient and led to the clearance of foreign material, DCs have been suggested to phagocytose only to an extent that is necessary to initiate the immune response (18).

Coating of MPs with IgG resulted in even more hydrophilic surfaces than BSA-coated MPs with comparable surface charge but led to more pronounced phagocytosis, which was comparably efficient in both DCs and M Φ . This may be explained by the interaction of the IgG-coated MPs with Fc receptors, which are abundantly expressed on the cell membrane of both DCs and M Φ , and mediate efficient receptor-mediated phagocytosis (15,48–50).

The strong phagocytosis of hydrophilic polyamine-coated MPs by DCs and M Φ is suggested to be caused by their strongly positive surface charge, which was demonstrated to be independent of the molecular weight or the chemical structure of the polyamines used in this study. The ionic attraction between the positively charged MPs and the negatively charged cell surface of the cells is likely to represent a strong stimulus that initiates binding and subsequent internalization (51).

Two principal mechanisms have been discussed to explain the internalization of MPs by phagocytic cells (20). For cationic MPs, we observed active pseudopod advancement engulfing the MPs, which is in analogy to the zipper mechanism and resulted in the formation of tightly apposed phagosomes. After the zipper mechanism, ingestion occurs by sequential engagement of a phagocyte's membrane against the MPs surface. Pseudopod advancement proceeds no further than receptor-ligand interactions permit and is probably related to a high affinity of the cell membrane to the particle surface. This could be induced by involvement of a receptor-ligand interaction, such as with IgG-opsonized or IgG-coated particles, which were actively engulfed by large protrusions, ending up in tightly apposed phagosomes (20). Alternatively, a high affinity of the particle surface to the cell membrane, such as for hydrophobic or positively charged particles, may result in a similar effect.

In contrast, hydrophilic BSA-coated MPs were phagocytosed without formation of pseudopods and ended up in loosely apposed phagosomes. This is in agreement with findings by others (21) and suggests phagocytosis in DCs and M Φ to occur according to the trigger mechanism (20). In this case, the particle would be ingested by a sinking-in-to-the-cell-like manner in loose contact to the phagosomal membrane.

Phagocytosed material ends up in phagosomes where it is then subject to several "fusion and fission" processes between phagosomes and lysosomes in order to exchange membrane constituents and vesicular contents (52). Thereby, the phagosome matures and acquires enzymes and membrane bound proton pumps, which are typically associated with lysosomes leading to a significant acidification of the matured phagosome (34,36–39). However, phagosomal maturation has been demonstrated to be inhibited depending on the type of phagocytosed MPs (21). Particularly, hydrophobic MPs were engulfed in tightly fitting phagosomes inhibiting phagosomal maturation. Protein-coated and hydrophilic MPs, however, were found to display loose interaction with the phagosomal membrane allowing rapid fusion with lysosomes (21). These observations are in accordance with our findings on protein-coated MPs carrying hydrophilic and negatively charged surfaces. Moreover, phagocytosed BSA- and IgG-coated MPs were found to end up in more acidic microenvironments of pH 4.6 to 5.1, indicating matured phagosomes. In contrast, we found hydrophilic polyamine-coated cationic MPs to be engulfed in tightly fitting phagosomes with a significantly less

acidic microenvironmental pH (6.0–6.8) as compared with protein-coated MPs. Phagosomal buffering, potentially followed by delayed phagosomal maturation, is one way to explain the minor acidification through cationic, polyamine-coated MP vs. the pronounced acidification with anionic, protein-coated MP (Table II). Another hypothesis is the polyamine-induced rupture of the endosomal membrane, which has been previously demonstrated to lead to the endosomal escape of PEI-associated material into the cytosol (26). According to the proton sponge hypothesis introduced by Behr (26), extensive buffering of the phagosome may even provoke ongoing proton transport by membrane-bound proton pumps and is followed by water influx. Finally, rupture of the phagosomal membrane and escape of the material entrapped in the phagosomes into the cytosol could be the consequence (26).

Based on our findings, we suggest maturation of phagosomes containing cationic MPs to be inhibited because of ionic interactions with the negatively charged phagosomal membrane. Besides, the investigated polyamines are likely to delay phagosomal acidification because of their buffering capacity (26). However, there was no visible evidence for phagosomal escape. The majority of the phagocytosed cationic MP observed in our study were coated by a tight phagosomal membrane even after 4 h of incubation and displayed no significant membrane disruption.

In summary, although hydrophilic, cationic MPs were efficiently phagocytosed by DCs, exceeding even the efficiency of receptor-mediated internalization of IgG-coated MPs. Electrostatic attraction between the positively charged MP surface and the negatively charged cell surface is likely to mediate binding and subsequent internalization. Phagocytosis was initiated by pseudopod advancement and led to the formation of phagosomes with a tightly apposed phagosomal membrane in a zipper-like manner. Furthermore, we found the intracellular pH in the microenvironment of cationic MPs to be significantly less acidic compared with the lower pH with other protein-coated MPs. This may be explained by the tight fit of the phagosomal membrane, which is suggested to lead to the inhibition of phagosomal maturation. Alternatively, intraphagosomal buffering by cationic coatings is likely to contribute to the reduced acidification and could also lead to delayed phagosomal maturation. In summary, the properties of cationic MPs to strongly enhance phagocytosis by DCs in combination with a delayed phagosomal maturation may hold promise for the intracellular delivery of immunomodulating therapeutics, which must be protected against lysosomal degradation to maintain their activity.

ACKNOWLEDGMENT

This work was supported by grants #4037-55144 from the Swiss National Research Foundation. Furthermore, we thank Dr. Ernst Wehrli and Dr. Markus Müller for their excellent help in electron microscopy.

REFERENCES

1. S. Raychaudhuri and K. L. Rock. Fully mobilizing host defense: building better vaccines. *Nat. Biotech.* **16**:1025–1031 (1998).
2. E. Walter, D. Dreher, M. Kok, L. Thiele, S. G. Kiama, P. Gehr, and H. P. Merkle. Hydrophilic poly(DL-lactide-co-glycolide) microspheres for the delivery of DNA to human-derived macrophages and dendritic cells. *J. Control. Release* **76**:149–168 (2001).
3. S. Prior, B. Gander, N. Blarer, H. P. Merkle, M. L. Subria, J. M. Irache, and C. Gamazo. In vitro phagocytosis and monocyte-macrophage activation with poly(lactide) and poly(lactide-co-glycolide) microspheres. *Eur. J. Pharm. Sci.* **15**:197–207 (2002).
4. J. Banchereau, F. Briere, C. Caux, J. Davoust, S. Lebecqque, Y. J. Liu, B. Pulendran, and K. Palucka. Immunobiology of dendritic cells. *Annu. Rev. Immunol.* **18**:767–811 (2000).
5. A. Aderem and D. M. Underhill. Mechanisms of phagocytosis in macrophages. *Annu. Rev. Immunol.* **17**:593–623 (1999).
6. J. Banchereau and R. M. Steinman. Dendritic cells and the control of immunity. *Nature* **392**:245–252 (1998).
7. F. D. Finkelman, A. Lees, R. Birnbaum, W. C. Gause, and S. C. Morris. Dendritic cells can present antigens in vivo in a tolerogenic or immunogenic fashion. *J. Immunol.* **157**:1406–1414 (1996).
8. Y. Men, H. Tamber, R. Audran, B. Gander, and G. Corradin. Induction of a cytotoxic T lymphocyte response by immunization with a malaria specific CTL peptide entrapped in biodegradable polymer microspheres. *Vaccine* **15**:1405–1412 (1997).
9. K. Peter, Y. Men, G. Pantaleo, B. Gander, and G. Corradin. Induction of a cytotoxic T-cell response to HIV-1 proteins with short synthetic peptides and human compatible adjuvants. *Vaccine* **19**:4121–4129 (2001).
10. Z. Shen, G. Reznikoff, G. Dranoff, and K. L. Rock. Cloned dendritic cells can present exogenous antigens on both MHC class I and class II molecules. *J. Immunol.* **158**:2723–2730 (1997).
11. M. Svensson, B. Stockinger, and M. J. Wick. Bone marrow-derived dendritic cells can process bacteria for MHC-I and MHC-II presentation to T cells. *J. Immunol.* **158**:4229–4236 (1997).
12. C. Scheicher, M. Mehlig, H. P. Dienes, and K. Reske. Uptake of microparticle-adsorbed protein antigen by bone marrow-derived dendritic cells results in up-regulation of interleukin-1 alpha and interleukin-12 p40/p35 and triggers prolonged, efficient antigen presentation. *Eur. J. Immunol.* **25**:1566–1572 (1995).
13. M. Kovacsovic-Bankowski and K. L. Rock. A phagosome-to-cytosol pathway for exogenous antigens presented on MHC class I molecules. *Science* **267**:243–246 (1995).
14. L. Thiele, B. Rothen-Rutishauser, S. Jilek, H. Wunderli-Allenspach, H. P. Merkle, and E. Walter. Evaluation of particle uptake in human blood monocyte-derived cells in vitro. Does phagocytosis activity of dendritic cells measure up with macrophages? *J. Control. Release* **76**:59–71 (2001).
15. Y. Tabata and Y. Ikada. Phagocytosis of polymer microspheres by macrophages. *Adv. Polymer Sci.* **94**:107–141 (1990).
16. H. Ayhan, A. Tuncel, N. Bor, and E. Piskin. Phagocytosis of monosize polystyrene-based microspheres having different size and surface properties. *J. Biomater. Sci.* **7**:329–342 (1995).
17. M. Singh, M. Briones, G. Ott, and D. O'Hagan. Cationic microparticles: a potent delivery system for DNA vaccines. *Proc. Natl. Acad. Sci. USA* **97**:811–816 (2000).
18. S. G. Kiama, L. Cochand, L. Karlsson, L. P. Nicod, and P. Gehr. Evaluation of phagocytic activity in human monocyte-derived dendritic cells. *J. Aerosol Med.* **14**:289–299 (2001).
19. C. R. Sousa and J. M. Austyn. Phagocytosis of antigens by Langerhans cells. *Adv. Exp. Med. Biol.* **329**:199–204 (1993).
20. J. A. Swanson and S. C. Baer. Phagocytosis by zippers and triggers. *Trends Cell Biol.* **5**:89–93 (1995).
21. C. De Chastellier and L. Thilo. Phagosome maturation and fusion with lysosomes in relation to surface property and size of the phagocytic particle. *Eur. J. Cell Biol.* **74**:49–62 (1997).
22. J. A. Swanson and C. Watts. Macropinocytosis. *Trends Cell Biol.* **5**:424–428 (1995).
23. E. Walter and H. P. Merkle. Microparticle-mediated transfection of non-phagocytic cells in vitro. *J. Drug Target.* **10**:11–21 (2002).
24. K. S. Denis-Mize, M. Dupuis, M. L. MacKichan, M. Singh, B. Doe, D. O'Hagan, J. B. Ulmer, J. J. Donnelly, D. M. McDonald, and G. Ott. Plasmid DNA adsorbed onto cationic microparticles mediates target gene expression and antigen presentation by dendritic cells. *Gene Ther.* **7**:2105–2112 (2000).
25. M. J. Mahoney and W. M. Saltzman. Transplantation of brain cells assembled around a programmable synthetic microenvironment. *Nat. Biotech.* **19**:934–939 (2001).

26. J. P. Behr. Gene transfer with amino lipids and amino polymers. *Compt. Rend. Seanc. Soc. Biol.* **190**:33–38 (1996).
27. A. Lorenzen and S. W. Kennedy. A fluorescence-based protein assay for use with a microplate reader. *Anal. Biochem.* **214**:346–348 (1993).
28. T. Arvinte, A. Cudd, and A. F. Drake. The structure and mechanism of formation of human calcitonin fibrils. *J. Biol. Chem.* **268**:6415–6422 (1993).
29. R. H. Müller, S. S. Davis, L. Illum, and E. Mak. Particle Charge and Surface Hydrophobicity of Colloidal Carriers. In G. Gregoriades, J. Senior, and G. Poste (eds.), *Targeting of drugs with synthetic system*, Plenum, New York 1986, pp. 239–263.
30. F. Sallusto, M. Cella, C. Danieli, and A. Lanzavecchia. Dendritic cells use macropinocytosis and the mannose receptor to concentrate macromolecules in the major histocompatibility complex class II compartment: downregulation by cytokines and bacterial products. *J. Exp. Med.* **182**:389–400 (1995).
31. F. Gantner, R. Kupferschmidt, C. Schudt, A. Wendel, and A. Hatzelmann. In vitro differentiation of human monocytes to macrophages: change of PDE profile and its relationship to suppression of tumour necrosis factor- α release by PDE inhibitors. *Br. J. Pharmacol.* **121**:221–231 (1997).
32. L. Cochand, P. Isler, F. Songeon, and L. P. Nicod. Human lung dendritic cells have an immature phenotype with efficient mannose receptors. *Am. J. Respir. Cell Mol. Biol.* **21**:547–554 (1999).
33. J. M. Coco-Martin, J. W. Oberink, T. A. van der Velden-de Groot, and E. C. Beuvery. Viability measurements of hybridoma cells in suspension cultures. *Cytotechnology* **8**:57–64 (1992).
34. M. J. Geisow. Fluorescein conjugates as indicators of subcellular pH. A critical evaluation. *Exp. Cell Res.* **150**:29–35 (1984).
35. G. P. Downey, R. J. Botelho, J. R. Butler, Y. Moltyaner, P. Chien, A. D. Scheiber, and S. Grinstein. Phagosomal maturation, acidification, and inhibition of bacterial growth in nonphagocytic cells transfected with Fc γ RIIA receptors. *J. Biol. Chem.* **274**:28436–28444 (1999).
36. R. H. Muller. *Colloidal Carriers for Controlled Drug Delivery and Targeting*. Wissenschaftliche Verlagsgesellschaft Stuttgart, 1990.
37. B. Poole and S. Ohkuma. Effect of weak bases on the intralysosomal pH in mouse peritoneal macrophages. *J. Cell Biol.* **90**:665–669 (1981).
38. S. Ohkuma, J. Chudzik, and B. Poole. The effects of basic substances and acidic ionophores on the digestion of exogenous and endogenous proteins in mouse peritoneal macrophages. *J. Cell Biol.* **102**:959–966 (1986).
39. P. Erbacher, J. S. Remy, and J. P. Behr. Gene transfer with synthetic virus-like particles via the integrin-mediated endocytosis pathway. *Gene Ther.* **6**:138–145 (1999).
40. S. E. Fong, P. Smanik, M. C. Smith, and S. R. Jaskunas. Cationic liposome-mediated uptake of human immunodeficiency virus type 1 Tat protein into cells. *J. Virol. Methods* **66**:149–157 (1997).
41. Y. Tabata and Y. Ikada. Effect of the size and surface charge of polymer microspheres on their phagocytosis by macrophage. *Bio-materials* **9**:356–362 (1988).
42. F. M. Griffin, J. A. Griffin, J. E. Leider, and S. C. Silverstein. Studies on the mechanism of phagocytosis. I. Requirements for circumferential attachment of particle-bound ligands to specific receptors on the macrophage plasma membrane. *J. Exp. Med.* **142**:1263–1282 (1975).
43. F. M. Griffin, J. A. Griffin, and S. C. Silverstein. Studies on the mechanism of phagocytosis. II. The interaction of macrophages with anti-immunoglobulin IgG-coated bone marrow-derived lymphocytes. *J. Exp. Med.* **144**:788–809 (1976).
44. A. M. Torche, P. Le Corre, E. Albina, A. Jestin, and R. Le Verge. PLGA microspheres phagocytosis by pig alveolar macrophages: influence of poly(vinyl alcohol) concentration, nature of loaded-protein and copolymer nature. *J. Drug Target.* **7**:343–354 (2000).
45. D. R. Absolom. Opsonins and dysopsonins: an overview. *Methods Enzymol.* **132**:281–318 (1986).
46. K. Inaba, M. Inaba, M. Naito, and R. M. Steinman. Dendritic cell progenitors phagocytose particulates, including bacillus Calmette-Guerin organisms, and sensitize mice to mycobacterial antigens in vivo. *J. Exp. Med.* **178**:479–488 (1993).
47. K. Matsuno, T. Ezaki, S. Kudo, and Y. Uehara. A life stage of particle-laden rat dendritic cells in vivo: their terminal division, active phagocytosis, and translocation from the liver to the draining lymph. *J. Exp. Med.* **183**:1865–1878 (1996).
48. A. Regnault, D. Lankar, V. Lacabanne, A. Rodriguez, C. Thery, M. Rescigno, T. Saito, S. Verbeek, C. Bonnerot, P. Ricciardi-Castagnoli, and S. Amigorena. Fc γ receptor-mediated induction of dendritic cell maturation and major histocompatibility complex class I-restricted antigen presentation after immune complex internalization. *J. Exp. Med.* **189**:371–380 (1999).
49. D. Maurer, E. Fiebiger, B. Reiningger, C. Ebner, P. Petzelbauer, G. P. Shi, H. A. Chapman, and G. Stingl. Fc epsilon receptor I on dendritic cells delivers IgE-bound multivalent antigens into a cathepsin S-dependent pathway of MHC class II presentation. *J. Immunol.* **161**:2731–2739 (1998).
50. N. A. Fanger, D. Voigtlaender, C. Liu, S. Swink, K. Wardwell, J. Fisher, R. F. Graziano, L. C. Pfefferkorn, and P. M. Guyre. Characterization of expression, cytokine regulation, and effector function of the high affinity IgG receptor Fc gamma RI (CD64) expressed on human blood dendritic cells. *J. Immunol.* **158**:3090–3098 (1997).
51. L. Josephson, C. H. Tung, A. Moore, and R. Weissleder. High-efficiency intracellular magnetic labeling with novel superparamagnetic-Tat peptide conjugates. *Bioconjug. Chem.* **10**:186–191 (1999).
52. M. Desjardins. Biogenesis of phagolysosomes: the 'kiss and run' hypothesis. *Trends Cell Biol.* **5**:183–187 (1995).